Utility of fiducial markers for target positioning in proton radiotherapy of oesophageal carcinoma

Apolle, R.; Brückner, S.; Frosch, S.; Rehm, M.; Thiele, J.; Valentini, C.; Lohaus, F.; Babatz, J.; Aust, D. E.; Hampe, J.; Troost, E. G. C.;

Originally published:

January 2019

Radiotherapy and Oncology 133(2019), 28-34

DOI: https://doi.org/10.1016/j.radonc.2018.12.016

Perma-Link to Publication Repository of HZDR:

https://www.hzdr.de/publications/Publ-27921

Utility of fiducial markers for target positioning in proton radiotherapy of oesophageal carcinoma

Rudi Apolle[1,2]; Stefan Brückner[3]; Susanne Frosch[4]; Maximilian Rehm[4]; Julia Thiele[2,4]; Chiara Valentini[2,4]; Fabian Lohaus[2,4]; Jana Babatz[3]; Daniela E. Aust[5], Jochen Hampe[3]; Esther G.C. Troost[1,2,4,6,7]

[1]Helmholtz-Zentrum Dresden - Rossendorf, Institute of Radiooncology – OncoRay, Dresden, Germany

[2]OncoRay – National Center for Radiation Research in Oncology, Faculty of Medicine and University Hospital Carl Gustav Carus, Technische Universität Dresden, Helmholtz-Zentrum Dresden - Rossendorf, Dresden, Germany

[3]Department of Internal Medicine I, University Hospital Carl Gustav Carus, Dresden, Germany

[4]Department of Radiotherapy and Radiation Oncology, Faculty of Medicine and University Hospital Carl Gustav Carus, Technische Universität Dresden, Dresden, Germany

[5]Institute for Pathology and Tumour and Normal Tissue Bank of the University Cancer Center (UCC), University Hospital Carl Gustav Carus, Medical Faculty, Technische Universität Dresden, Dresden, Germany

[6]German Cancer Consortium (DKTK), Partner Site Dresden, and German Cancer Research Center (DKFZ), Heidelberg, Germany

[7]National Center for Tumor Diseases (NCT), Partner Site Dresden, Germany: German Cancer Research Center (DKFZ), Heidelberg, Germany; Faculty of Medicine and University Hospital Carl Gustav Carus, Technische Universität Dresden, Dresden, Germany, and; Helmholtz Association / Helmholtz-Zentrum Dresden - Rossendorf (HZDR), Dresden, Germany

Corresponding author:
Rudi Apolle, MSc
OncoRay, National Center for Radiation Research in Oncology
Händelallee 26
01309 Dresden, Germany
Telephone: +49-(0)351-458-6532
E-mail: rudi.apolle1@oncoray.de
ORCID: 0000-0002-1375-0498

Abstract

Background and purpose

Oesophageal mobility relative to bony anatomy is a major source of geometrical uncertainty in proton radiotherapy of oesophageal carcinoma. To mitigate this uncertainty we investigated the use of implanted fiducial markers for direct target verification in terms of safety, visibility, and stability.

Materials and methods

A total of 19 helical gold markers were endoscopically implanted in ten patients. Their placement at the proximal and distal tumour borders was compared to tumour demarcations derived from [18F]Fluorodeoxyglucose positron emission tomography, their visibility quantified via the contrast-to-noise ratio on daily orthogonal X-ray imaging, and their mobility relative to bony anatomy analysed by means of retrospective triangulation.

Results

Marker implantation proceeded without complications, but the distal tumour border could not be reached in two patients. Marker locations corresponded reasonably well with metabolic tumour edges (mean: 5.4 mm more distally). Marker visibility was limited but mostly sufficient (mean contrast-to-noise ratio: 1.5), and sixteen markers (84%) remained in situ until the end of treatment. Overall, marker excursions from their planned position were larger than 5(10) mm in 59(17)% of all analysed fractions. On one occasion severe target displacement was only identified via markers and was corrected before treatment delivery.

Conclusion

Implanted helical gold fiducial markers are a safe and reliable method of providing target-centric positioning verification in proton beam therapy of oesophageal carcinoma.

Key words

oesophageal carcinoma, proton therapy, image-guided radiotherapy, fiducial markers.

Introduction

Tri-modality treatment consisting of neo-adjuvant radiochemotherapy (nRCT) followed by surgery is standard of care for resectable locally advanced oesophageal carcinoma. Results of the CROSStudy [1, 2] represent a major improvement over previous investigations, with meta-analyses of trials conducted in the three decades leading up to CROSS showing no significant or limited benefit [3,4]. This advance is likely a reflection of improved procedures in all involved specialties (radiology, nuclear medicine, medical and surgical oncology), as well as advances in radiotherapy (RT). CROSS was among the first trials to exclusively utilise three-dimensional conformal RT, which is endowed with an increased ability to spare critical thoracic structures surrounding the oesophagus, e.g. the heart and lungs, when compared to earlier techniques. The associated reduction of the likelihood of cardio-pulmonary complications might play a major role in the increase of overall survival associated with modern tri-modality treatment.

In an attempt to further improve outcome after nRCT in oesophageal cancer patients or/and to pave the way to organ-preserving RCT employing higher radiation doses, particle therapy, in particular using protons, is the focus of attention. Proton therapy (PT) offers unique dosimetric characteristics, which improve dose conformality at distal field edges where maximum dose deposition at the Bragg peak is followed by a sharp dose decline. While there is currently no data from randomised controlled trials comparing PT to photon-based RT techniques for oesophageal cancer, propensity-matched retrospective investigations have shown better survival rates in the primary setting and reduced postoperative complications in nRCT when delivering PT [5,6].

However, PT introduces geometrical uncertainties beyond those known from photon RT. The acuity of the distal dose fall-off and the underlying physical mechanism make it susceptible to changes in patient anatomy. Unless these uncertainties can be mitigated without introducing excessive safety margins, it will be hard to translate the physical advantages of PT into clinical benefit. Target positioning, in particular, is one aspect of treatment, which needs to be tightly controlled.

Oesophageal tumours show pronounced variability in daily target position, as well as significant intra-fractional motion [7-9]. Many PT facilities utilise orthogonal X-ray imaging for daily patient setup based on bony anatomy, but are unable to provide target-centric positioning due to its inherent lack of soft-tissue contrast. Implanted radiopaque fiducial markers can overcome this limitation and enable verification of target positioning to complement bony setup. They also allow for retrospective analyses of residual target positioning errors, which can be used to tailor safety margins to the uncertainties encountered at a particular department.

Here we report on the experience with one type of commercially available fiducial marker in ten patients with oesophageal cancer treated with neoadjuvant or primary RCT using protons. Apart from safety, we analysed marker visibility on daily X-ray imaging, their stability, and mobility. Based thereupon we discuss a marker-based target position verification procedure, which can be straightforwardly implemented in routine clinical practice.

Materials and methods

Patient cohort

Patients were recruited between June 2017 and July 2018 with the aim of investigating marker implantation safety. The primary eligibility criterion was a histologically confirmed oesophageal carcinoma potentially amenable to curative treatment. This included locally advanced cases, as well as early-stage disease unsuitable for primary resection. Exclusion criteria were complete stenosis of the oesophagus hampering marker implantation or the presence of distant metastases leading to palliative treatment. All patients underwent routine staging according to the AJCC/UICC manual (8th edition)[10]. [18F]Fluorodeoxyglucose positron emission tomography (FDG-PET) was preferably scheduled after marker implantation. The investigation was approved by our university's medical ethics committee (EK148042017) and filed with the German registry of clinical trials (DRKS00011886). All patients provided written informed consent.

Fiducial markers

Marker implantation was guided by endoscopic ultrasound (EUS) and performed under conscious sedation and continuous monitoring of vital signs by three experienced endosonographers. One type of flexible, coil-shaped gold marker (VisiCoil^{TM}, IBA Dosimetry, Schwarzenbruck, Germany; diameter 0.35 mm, length 5/10 mm) was placed via 22-gauge needles [11]. Two markers were implanted at the upper and lower borders of the tumour, respectively, if both were accessible. An additional marker could be inserted into the healthy oesophagus facing non-circumferential tumours at mid-position. Colour and power Doppler imaging were used to identify a safe insertion window devoid of intervening blood vessels, wherein the endoscopic needle was then inserted submucosally under EUS guidance. After marker release, its location was confirmed using fluoroscopy and the implantation site inspected for oesophageal bleeding. Patients were monitored for 4 hours afterwards.

Pre-treatment imaging

Patients with tumours in the middle or lower third of the oesophagus were immobilised in a vacuum cushion, while a thermoplastic mask covering the head and shoulder region was used in one patient with a tumour affecting the upper third. Patients breathed freely during imaging and subsequent PT. All patients underwent a diagnostic FDG-PET scan (5 mm slice thickness, 4 mm in-plane resolution, BioGraph 16; Siemens Healthineers, Erlangen, Germany) and a 4D CT for RT planning purposes

(pCT; 120 kVp, 2 mm slice thickness, 1mm in-plane resolution, Somatom Definition AS, Siemens Healthineers). PET-based gross tumour volumes (GTV) comprising all voxels exceeding 40% of the hottest voxel's signal were generated for comparisons of metabolic lesion extent with marker locations.

Target volume definition, radiation treatment and chemotherapy

Regions of interest (ROIs) were drawn around fiducial markers on the pCT and isotropically expanded by 3–5 mm to be later projected onto digitally reconstructed radiographs (DRRs) for target verification. GTV delineation was primarily guided by FDG-PET data co-registered to the pCT, but incorporated all available diagnostic information. PET-positive nodes were included in a separate nodal GTV. The clinical target volume (CTV) was derived by expanding the GTV 30(10) mm longitudinally(laterally), with subsequent editing for anatomical boundaries. For tumours demonstrating large mobility on 4D-pCT, the CTVs were further expanded into ITVs by motion-dependent margins ranging from 4–10 mm (median: 5). Organs at risk comprising the heart, lungs, spinal cord, stomach, spleen, liver, or kidneys were delineated on the time-averaged pCT.

Treatment plans utilised two to three passively scattered or actively scanned proton fields, delivered with a Proteus PLUS system (IBA Proton Therapy, Louvain-La-Neuve, Belgium) installed at University ProtonTherapy Dresden. Instead of using a PTV, margins around the CTV/ITV allowing for a 3.5% range uncertainty and additional static margins of 2(3) mm in beam direction(laterally) were applied. Prescribed doses were 40 GyE or 60–66 GyE for nRCT and primary RT, respectively, delivered in 2GyE fractions. Concurrent chemotherapy was administered according to the CROSS protocol and consisted of a paclitaxel/carboplatin doublet delivered once weekly (dosage: 50 mg/m^2 and AUC2, respectively).

Per-treatment imaging and marker-based target position verification

The gantry at University ProtonTherapy Dresden is equipped with a robotic patient couch with six degrees of freedom (KUKA, Augsburg, Germany), an in-room CT on-rails whose specifications match that of the scanner used for planning purposes, and a gantry-mounted orthogonal X-ray system (resolution approximately 0.2 mm at the isocentre). The latter was used to capture images in treatment position before each fraction using pre-set defaults for tube potential and current-time-product (80 kV/160 mAs for sagittal, 95 kV/50 mAs for coronal views).

In clinical routine, patient setup begins with external alignment of surface marks to the in-room laser system. Thereafter, X-rays are acquired and digitally compared to DRRs derived from the pCT. A setup correction is calculated from a manual registration between the two image pairs based on bony anatomy (VeriSuite, MedCom, Darmstadt, Germany) including shifts and rotations. Finally, for oesophageal cancer patients, target positioning is verified with the aid of fiducial markers, through their associated ROIs projected onto the DRRs. These should contain the marker to verify its location to within 3–5 mm. Should target misalignment be detected, patient positioning is repeated and/or an in-room control CT (cCT) acquired to investigate its cause.

Retrospective analysis of orthogonal X-ray images

Marker visibility was quantified via the contrast-to-noise ratio (CNR). Two ROIs were constructed around each marker: one containing only the marker projection, the other immediately surrounding, but excluding, it (Fig.1). The CNR was then computed as the absolute difference in mean pixel values in each ROI divided by their combined standard deviation. Commonly employed minimum CNR thresholds for visibility range from 1–2 [12,13].

Markers were manually located in each image pair and their location in 3D reconstructed by triangulation (Algorithm 12.1 in [14]). Two anatomical reference points (vertebral landmarks) per patient were similarly reconstructed, in order to compare findings between projection and tomographic imaging. Triangulation errors were estimated from the distances of closest approach between back-projections of corresponding 2D points (Fig.1). This measure is primarily sensitive to longitudinal discrepancies, so the 90th percentile of a marker's approach distances in all fractions was assigned as its isotropic triangulation error.

Target displacements relative to the pCT were decomposed into their systematic and statistical components in the manner popularised by van Herk et al. [15] (Σ and σ). Displacements in the three cardinal directions were investigated individually, as were the corresponding 3D-vector (Euclidean) distances.

Statistical analysis

Parameter-free tests were used to compare differently grouped variables, since their distributions could not be assumed. Friedman tests were used to compare marker displacements in the three cardinal directions, and Kruskal-Wallis tests to compare unmatched groupings. Specifically, comparisons of systematic and statistical components of mobility respectively probe differences

between individual markers' absolute mean displacement, and differences in the standard deviations of their displacement (as per [9]). Monotonic relationships between two variables were probed by Spearman rank correlation. A significance criterion of $p<0.05$ applies throughout.

Results

Ten consecutive patients were enrolled in the study (Tbl. 1). Eight patients received nRCT, while the remaining two were treated primarily. One (patient 1) was treated for a recurrence of an adenocarcinoma of the gastrooesophageal junction resected two years prior, and the other (patient 9) was not suitable for resection due to a proximal tumour site. The latter patient also received elective treatment of the lower neck nodes up to 40 GyE due to infiltration of the upper oesophageal sphincter. The remaining patients had tumours affecting the middle (n=4) or lower (n=4) third of the oesophagus.

A total of 19 markers were implanted, and there were no periprocedural complications. The median interval between marker implantation and pCT acquisition was 1.5 days (range: 1–29). In two cases (patients 5 and 10) the distal tumour border was inaccessible by endoscope due to obstruction. One proximal marker fragmented at implantation and was subsequently lost (patient 9). Two further proximal markers of 5 mm length became dislodged before or during treatment (patients 1, 4). Figure 3 shows the sole instance of progressive marker migration, wherein it travelled more than 10mm in 10 fractions and was simultaneously deformed. The mean extent of primary gross disease on the pCT was 24.5 ml (range: 9.2–69.0) in volume and 47.6 mm (range: 20–80) in length.

Three patients received their FDG-PET-CT prior to marker implantation, for the remaining cases the median interval was 2.0 days (range: 1–6). Figure 2 provides an overview of longitudinal marker locations and their correspondence with FDG-PET-derived GTVs. The mean separation between marker positions and corresponding GTV borders was -5.4±8.1 mm (range: -21.5–7.5), with negative values indicating markers located more distally.

X-ray pairs could be retrieved for 211/223 fractions and the number of cCTs per patient ranged from 2–3. Markers were easily detected in (PET-)CT image sets, while visibility in X-ray images was generally limited but mostly sufficient. Markers were completely undetectable in sagittal views of the patient immobilised with a thermoplastic mask, reducing the number of analysable marker projection pairs to 307 out of a possible 446 if all patient had received two markers, which remained stable and visible throughout.

The overall mean CNR was 1.5±0.5 (range: 0.2–3.2) with 508(90)/614 marker projections satisfying a visibility criterion of CNR>1(2). Mean CNRs were 1.5±0.5 for sagittal and 1.5±0.5 for coronal projections (p=0.8), while values of 1.7±0.3, 1.7±0.5, and 1.4±0.4 were achieved with markers located in the upper, middle and lower third of the oesophagus, respectively ($p<0.01$).

Triangulation approach distances ranged from 0.0–6.0 mm (mean: 1.2±1.1) and showed no correlation with the combined CNR of both marker projections (p=0.2). Assigned triangulation

errors per marker ranged from 0.8–4.8 mm (mean: 2.4±1.2) and showed a dependence on marker site with mean values of 3.1±1.0 mm for the lower third of the oesophagus and 1.6±0.9 mm for the others ($p=0.01$).

Figure 4 shows the aggregate distributions of marker displacements alongside summary statistics. No significant differences in mobility were found with regard to marker location. When comparing directions of movement, significant differences were only found in the statistical component ($p<0.05$). Euclidean displacement exceeded 5(10) mm in 181(57)/307 cases. The most extreme instance of marker displacement is shown in Fig. 5 and features the proximal(distal) marker displaced by 17(31) mm. This prompted the acquisition of a cCT, which revealed an overlap of the planned and actual GTVs of merely 4% (Jaccard index: 0.02). The dosimetric impact would have been a reduction of the mean and near-min (D98%) doses by 6% and 47%, respectively.

Discussion

This investigation represents the first detailed utility analysis of VisiCoil™ fiducial markers in neoadjuvant or primary proton RCT of oesophageal carcinoma. Marker implantation proceeded without complications and all markers of the longer type (10 mm) remained stable throughout treatment. Marker visibility was oftentimes limited but mostly sufficient and marker positions could be triangulated for all but one patient.

The addition of FDG-PET to CT-based treatment planning has enabled more accurate definition of both primary and nodal GTVs in oesophageal cancer [16]. Its coarse spatial resolution limits sensitivity to superficial disease extension, however, as was observed in comparisons with resection specimen in laryngeal carcinoma [17]. Foley et al. [18] found improved assessment of local disease extent by EUS, and strongly recommend combining information from FDG-PET and EUS with the pCT. As shown in this study, fiducial markers placed under EUS-guidance support this approach by making endoscopic findings available on projective or tomographic X-ray imaging.

Marker visibility could be substantially improved through the optimisation of imaging parameters, as detailed by Chen et al. [12] in the context of prostate RT. They used an anthropomorphic phantom and determined the ratio of CNR to entrance skin exposure for varying combinations of tube potential and current-time-product for individual projection angles. The optimal settings they determined are likely not transferable to all patients, but could serve as a starting point for patient-specific optimisation. Care has to be taken, however, not to sacrifice the contrast of bony anatomy, since both patient setup and target verification need to be achieved simultaneously.

Mobility measurements were generally in good agreement with those by Jin et al. [9], who used a variety of fiducial markers and frequent cone-beam CT (CBCT) to study inter-fractional motion of oesophageal tumours. For their entire cohort of 65 markers (31 in the distal oesophagus) they measured $\Sigma(\sigma)$ as 2.9(2.4), 2.2(1.8), and 4.1(2.4) mm, for the lateral, sagittal, and axial directions, respectively. They report significant differences in both statistical and systematic components of movement when comparing cardinal directions, with highest mobility in the longitudinal direction. In our study, the distributions of marker displacements show some prominent outliers, which partially stem from fractions where positioning was ultimately established by cCT without repeating X-ray imaging. There is a sizeable systematic shift in the sagittal direction whose underlying cause has yet to be understood.

Metallic markers can cause severe dose shadows in ion beams. Several simulation and measurement studies (e.g. [19-21]) have shown dose deficits of up to 80%, depending on marker dimensions, material, orientation and position relative to the beams and their respective Bragg peaks. This has prompted the development of novel marker materials (e.g. carbon and liquid fiducial markers [22]), as well as the introduction of reduced material markers, such as VisiCoil^{TM}. Two studies included this marker type and diameter, measuring dose perturbations in mono-energetic proton or carbon ion beams [19] and at different positions in a spread-out proton Bragg peak [20]. Neither study reports observable dose perturbations for the 0.35 mm diameter VisiCoil^{TM} marker. Machiels et al. [23] compared this calibre of VisiCoil^{TM} to solid gold markers of similar outer dimensions finding superior stability for the helical design, thereby demonstrating that the favourably low material budget does not sacrifice stability. They recommend marker lengths >5mm for optimal stability, which is in line with our findings.

A natural alternative to marker-based targeting verification would be to locate the target natively in daily (CB)CTs. While technically achievable in some cases, the lack of soft tissue contrast makes direct target-to-target matching very difficult such that reliable surrogates need to be found [24]. The considerable excess dose to non-target structures over orthogonal X-ray imaging also needs to be considered.

Perhaps the most experience with fiducial markers has been gathered in photon RT of the prostate, where they have surpassed bony anatomy as reliable references for patient positioning under radiographic imaging [25]. The same might not be attainable in proton RT, since its correct application requires both target volumes and the surrounding anatomy to be in their planned configuration. Hence, our setup procedure is initially focused on bony anatomy as a surrogate for overall patient geometry, and then extended by direct targeting verification through fiducial markers. This has proven a straightforward and reliable approach, and become standard of care for PT of oesophageal carcinoma at our department. Since imaging and verification can be performed comparatively quickly, treatment preparation is only prolonged in cases of actual target displacement, which would otherwise have gone unnoticed and interfered with dose delivery.

In conclusion, implanted fiducial markers proved to be a valuable aid in target delineation and an effective tool for target-centric positioning verification in oesophageal carcinoma.

References

[1] Van Hagen P, Hulshof MCCM, Van Lanschot JJB, Steyerberg EW, Van Berge Henegouwen MI, Wijnhoven BPL, et al.. Preoperative chemoradiotherapy for esophageal or junctional cancer. N Engl J Med 2012;366:2074–84. doi:10.1056/NEJMoa1112088.

[2] Shapiro J, Van Lanschot JJB, Hulshof MCCM, Van Hagen P, Van Berge Henegouwen MI, Wijnhoven BPL, et al.. Neoadjuvant chemoradiotherapy plus surgery versus surgery alone for oesophageal or junctional cancer (CROSS): long-term results of a randomised controlled trial. Lancet Oncol 2015;16:1090–8. doi:10.1016/S1470-2045(15)00040-6.

[3] Gebski V, Burmeister B, Smithers BM, Foo K, Zalcberg J, Simes J. Survival benefits from neoadjuvant chemoradiotherapy or chemotherapy in oesophageal carcinoma: a meta-analysis. Lancet Oncol 2007;8: 226–34. doi:10.1016/S1470-2045(07)70039-6.

[4] Arnott S, Duncan W, Gignoux M, Hansen H, Launois B, Nygaard K, et al.. Preoperative radiotherapy for esophageal carcinoma. Cochrane Database Syst Rev 2005;CD001799. doi:10.1002/14651858.CD001799.pub2.

[5] Xi M, Xu C, Liao Z, Chang JY, Gomez DR, Jeter M, et al.. Comparative Outcomes After Definitive Chemoradiotherapy Using Proton Beam Therapy Versus Intensity Modulated Radiation Therapy for Esophageal Cancer: A Retrospective, Single-Institutional Analysis. Int J Radiat Oncol Biol Phys 2017;99:667–76. doi:10.1016/j.ijrobp.2017.06.2450.

[6] Lin S, Merrell K, Shen J, Verma V, Correa A, Wang L, et al.. Multi-institutional analysis of radiation modality use and postoperative outcomes of neoadjuvant chemoradiation for esophageal cancer. Radiother Oncol 2017;123:376–81. doi:10.1016/j.radonc.2017.04.013.

[7] Dieleman E, Senan S, Vincent A, Lagerwaard F, Slotman B, Van Sörnsen de Koste J. Four-dimensional computed tomographic analysis of esophageal mobility during normal respiration. Int J Radiat Oncol Biol Phys 2007;67:775–80. doi:10.1016/j.ijrobp.2006.09.054.

[8] Cohen R, Paskalev K, Litwin S, Price R, Feigenberg S, Konski A. Esophageal motion during radiotherapy: quantification and margin implications. Dis Esophagus 2010;23:473–9. doi:10.1111/j.1442-2050.2009.01037.x.

[9] Jin P, Van der Horst A, De Jong R, Van Hooft J, Kamphuis M, Van Wieringen N, et al.. Marker-based quantification of interfractional tumor position variation and the use of markers for setup verification in radiation therapy for esophageal cancer. Radiother Oncol 2015;117:412–8. doi:10.1016/j.radonc.2015.10.005.

[10] Amin MB, Edge S, Greene F, Byrd DR, Brookland RK, Washington MK, et al., editors. AJCC Cancer Staging Manual. 8th ed. New York: Springer; 2017.

[11] DiMaio C, Nagula S, Goodman K, Ho A, Markowitz A, Schattner M, et al.. EUS-guided fiducial placement for image-guided radiation therapy in GI malignancies by using a 22-gauge needle (with videos). Gastrointest Endosc 2010;71:1204–10. doi:10.1016/j.gie.2010.01.003.

[12] Chen Y, O'Connell J, Ko C, Mayer R, Belard A, McDonough J. Fiducial markers in prostate for kV imaging: quantification of visibility and optimization of imaging conditions. Phys Med Biol 2012;57:155–72. doi:10.1088/0031-9155/57/1/155.

[13] Luo W, Yoo S, Wu QJ, Wang Z, Yin F. Analysis of image quality for real-time target tracking using simultaneous kV-MV imaging. Med Phys 2008;35:5501–9. doi:10.1118/1.3002313.

[14] Hartley R, Zisserman A. Multiple View Geometry in Computer Vision. 2nd ed. New York: Cambridge University Press; 2004.
[15] Van Herk M. Errors and margins in radiotherapy. Semin Radiat Oncol 2004;14:52–64. doi:10.1053/j.semradonc.2003.10.003.
[16] Schreurs LMA, Busz DM, Paardekooper GMRM, Beukema JC, Jager PL, Van der Jagt EJ, et al.. Impact of 18-fluorodeoxyglucose positron emission tomography on computed tomography defined target volumes in radiation treatment planning of esophageal cancer: reduction in geographic misses with equal inter-observer variability: PET/CT improves esophageal target definition. Dis Esophagus 2010;23:493–501. doi:10.1111/j.1442-2050.2009.01044.x.
[17] Daisne J, Duprez T, Weynand B, Lonneux M, Hamoir M, Reychler H, et al.. Tumor volume in pharyngolaryngeal squamous cell carcinoma: comparison at CT, MR imaging, and FDG PET and validation with surgical specimen. Radiology 2004;233:93–100. doi:10.1148/radiol.2331030660.
[18] Foley KG, Morgan C, Roberts SA, Crosby T. Impact of Positron Emission Tomography and Endoscopic Ultrasound Length of Disease Difference on Treatment Planning in Patients with Oesophageal Cancer. Clin Oncol (R Coll Radiol) 2017;29:760–6. doi:10.1016/j.clon.2017.07.014.
[19] Habermehl D, Henkner K, Ecker S, Jäkel O, Debus J, Combs S. Evaluation of different fiducial markers for image-guided radiotherapy and particle therapy. J Radiat Res 2013;54:i61–8. doi:10.1093/jrr/rrt071.
[20] Giebeler A, Fontenot J, Balter P, Ciangaru G, Zhu R, Newhauser W. Dose perturbations from implanted helical gold markers in proton therapy of prostate cancer. J Appl Clin Med Phys 2009;10:2875.
[21] Newhauser W, Fontenot J, Koch N, Dong L, Lee A, Zheng Y, et al.. Monte Carlo simulations of the dosimetric impact of radiopaque fiducial markers for proton radiotherapy of the prostate. Phys Med Biol 2007;52:2937–52. doi:10.1088/0031-9155/52/11/001.
[22] Scherman Rydhög J, Perrin R, Jølck RI, Gagnon-Moisan F, Larsen KR, Clementsen P, et al.. Liquid fiducial marker applicability in proton therapy of locally advanced lung cancer. Radiother Oncol 2017;122:393–9. doi:10.1016/j.radonc.2016.12.027.
[23] Machiels M, Van Hooft J, Jin P, Van Berge Henegouwen MI, Van Laarhoven HM, Alderliesten T, et al.. Endoscopy/EUS-guided fiducial marker placement in patients with esophageal cancer: a comparative analysis of 3 types of markers. Gastrointest Endosc 2015;82:641–9. doi:10.1016/j.gie.2015.03.1972.
[24] Hawkins MA, Aitken A, Hansen VN, McNair HA, Tait DM. Cone beam CT verification for oesophageal cancer - impact of volume selected for image registration. Acta Oncol 2011;50:1183–90. doi:10.3109/0284186X.2011.572912.
[25] O'Neill AGM, Jain S, Hounsell AR, O'Sullivan JM. Fiducial marker guided prostate radiotherapy: a review. Br J Radiol 2016;89:20160296. doi:10.1259/bjr.20160296.

Table Headings

Table 1: Patient, tumour, and treatment characteristics.

Figure Captions

Figure 1: Overview of marker implantation, imaging techniques and analysis procedures. Top row, left to right: Endoscopic marker implantation showing full range of employed instruments; Correspondence of marker positions and metabolic tumour extent seen in FDG-PET-CT; Geometry of daily X-ray projection imaging. Bottom row: Left: Illustration of CNR extraction using marker and background ROIs for sagittal and coronal views of the same marker achieving good and poor visibility, respectively, based on a visibility criterion of CNR>1; Right: Illustration of triangulation procedure and determination of one marker's assigned isotropic triangulation error as the 90th percentile of the distribution of distances of closest approach between the back-projections of sagittal and coronal 2D marker positions towards their respective X-ray sources for that marker over all fractions.

Figure 2: Overview of longitudinal marker locations (triangles) and GTV lengths (columns). Data extracted from FDG-PET-CT (blue, GTV consists of all voxels whose value exceeds 40% of the lesion's hottest voxel) is compared to data from planning CTs (red, GTV contoured manually using co-registered PET data). Measurements are aligned by the proximal anatomical reference, while the distal references are shown as crosses. Please note: GTV based on FDG-PET is not shown for patient 1, due to a very weak PET-signal exacerbated by extensive metallic sutures. Some patients did not have a distal marker implanted (5, 10), experienced loss of the proximal marker before imaging (1), or had their PET acquired before implantation (4,5,7).

Figure 3: Marker positions over the course of treatment for a patient, whose proximal marker underwent progressive migration and deformation, as well as detailed views of the latter. A: Marker positions in cardinal directions for each fraction, as well as the corresponding Euclidean inter-marker distances. Dotted horizontal lines indicate the nominal 3mm verification threshold. B: Coronal views of the proximal marker for fractions 10, 13, 16, and 20. Each view is centred on the interface of thoracic vertebrae 5 and 6.

Figure 4: Distributions of inter-fractional marker displacements relative to their planned position in each of the cardinal directions, as well as their Euclidean combination. Distributions are shown as histograms (grey, 1mm binning). Summary statistics are drawn as coloured lines and printed underneath. Σ and σ refer to the decomposition of mobility measurements into systematic and random components as per [15]. Abbreviations: LAT, lateral; SAG, sagittal; AXL, axial; 3D, 3D vector (Euclidean) distance; post, posterior; ant, anterior; sup, superior; inf, inferior, std, standard deviation; iqr, inter-quartile range.

Figure 5: Marker positions over the course of treatment for a patient showing severe target displacement at one fraction, as well as detailed views of the latter. A: Marker positions in cardinal directions for each fraction, as well as the corresponding Euclidean inter-marker distances. Dotted horizontal lines indicate the nominal 3mm verification threshold. B: Coronal views for fractions 13 and 14 showing pronounced excursion of both markers to the right. Projections of GTVs delineated on the planning CT and a control CT are superimposed for comparison.

Table 1

Patient number	Age [years]	Tumour characteristics*		Gross tumour extent§		Fiducial markers		Implantation → Imaging		Treatment	
		Location	Classification	Volume [ml]	Length [mm]	Number	Lengths [mm]	pCT [days]	PET [days]¶	Fractions	cCTs
1	64	lower	rcT1a cN0	9.2	32	2→1†	5	4	4	30	2
2	52	lower	cT2 cN1	28.5	40	2	5,10	1	2	20	2
3	58	middle	cT3 cN1	10.4	32	2	10	4	4	20	2
4	62	lower	cT3 cN0	15.0	56	2→1‡	5	1	-15	20	2
5	57	middle	cT3 cN0	18.5	40	1	10	2	-34	20	3
6	55	lower	cT3 cN1	69.0	80	2	10	6	6	20	2
7	63	middle	cT3 cN0	27.1	68	2	10	1	-22	20	3
8	67	lower	cT3 cN1	14.1	40	2	10	1	1	20	2
9	61	upper	cT3 cN0	5.3	20	2→1‡†	10	29	2	33	2
10	74	middle	cT3 cN0	47.7	68	2‡‡	10	1	1	20	3

Abbreviations: (p/c)CT, (planning/control) computed tomography; PET, positron emission tomography.

Notes: *Determined according to AJCC/UICC guidelines. Location refers to affected third of the oesophagus; §From GTV delineations; ¶Negative values indicate that acquisition occured prior to marker implantation; †Proximal marker lost before pCT acquisition; ‡Proximal marker lost after 4th fraction; ‡†Proximal marker became fragmented at implantation and was lost after 7th fraction; ‡‡Both markers placed at proximal border.

Figure 1

Click here to download high resolution image

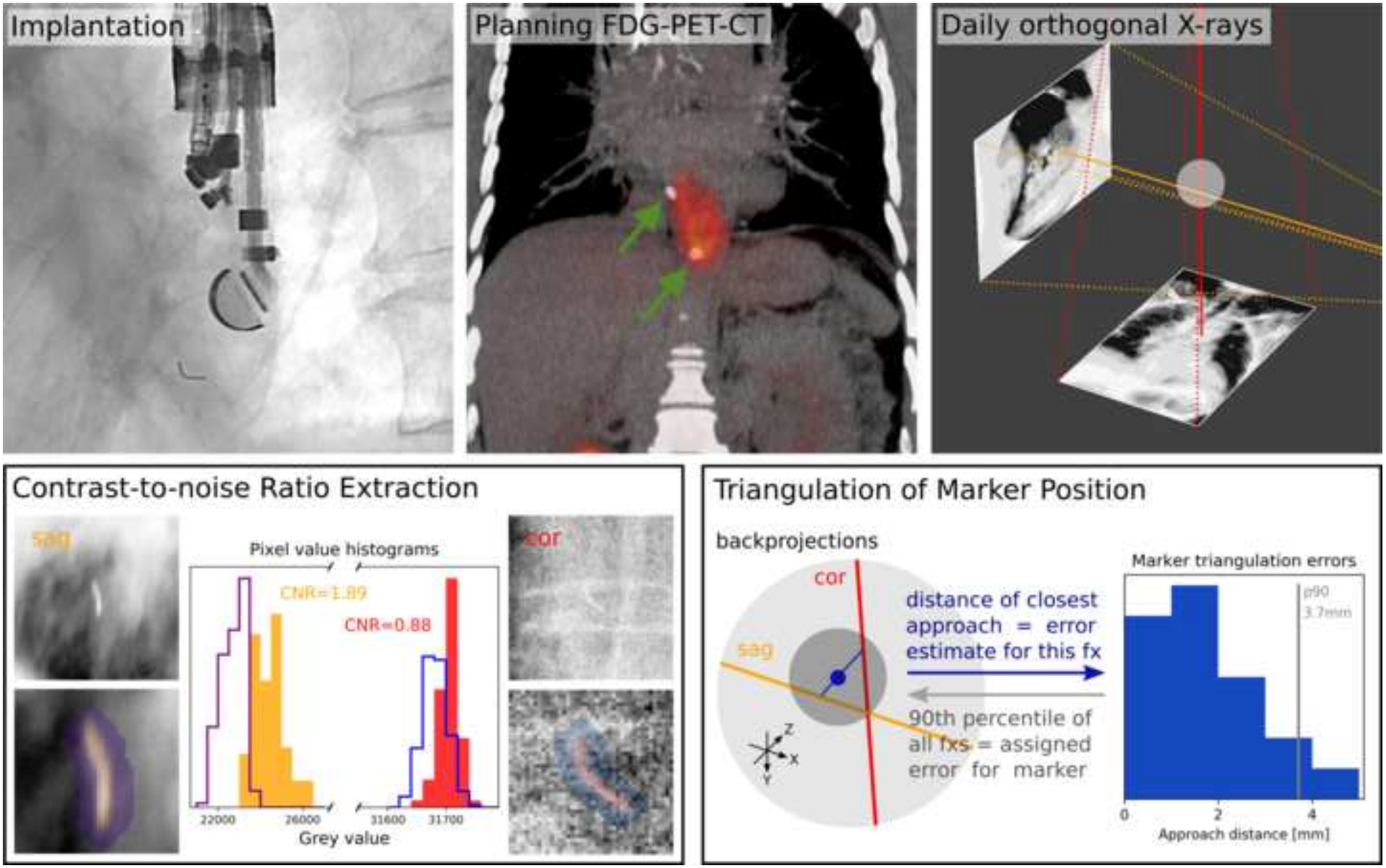

Figure 2

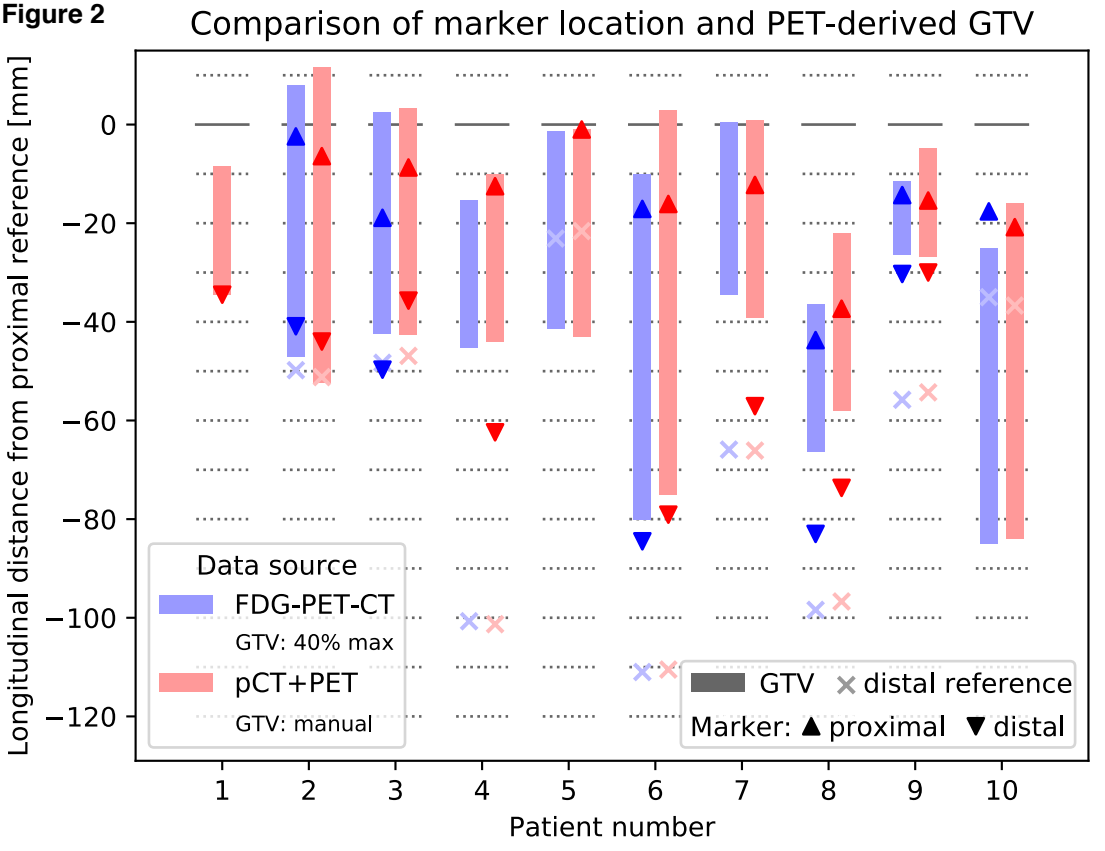
Comparison of marker location and PET-derived GTV
Longitudinal distance from proximal reference [mm]
0
−20
−40
−60
−80
−100
−120
1
2
3
4
5
6
7
8
9
10
Patient number
Data source
FDG-PET-CT
GTV: 40% max
pCT+PET
GTV: manual
GTV
distal reference
Marker: proximal distal

Figure 3

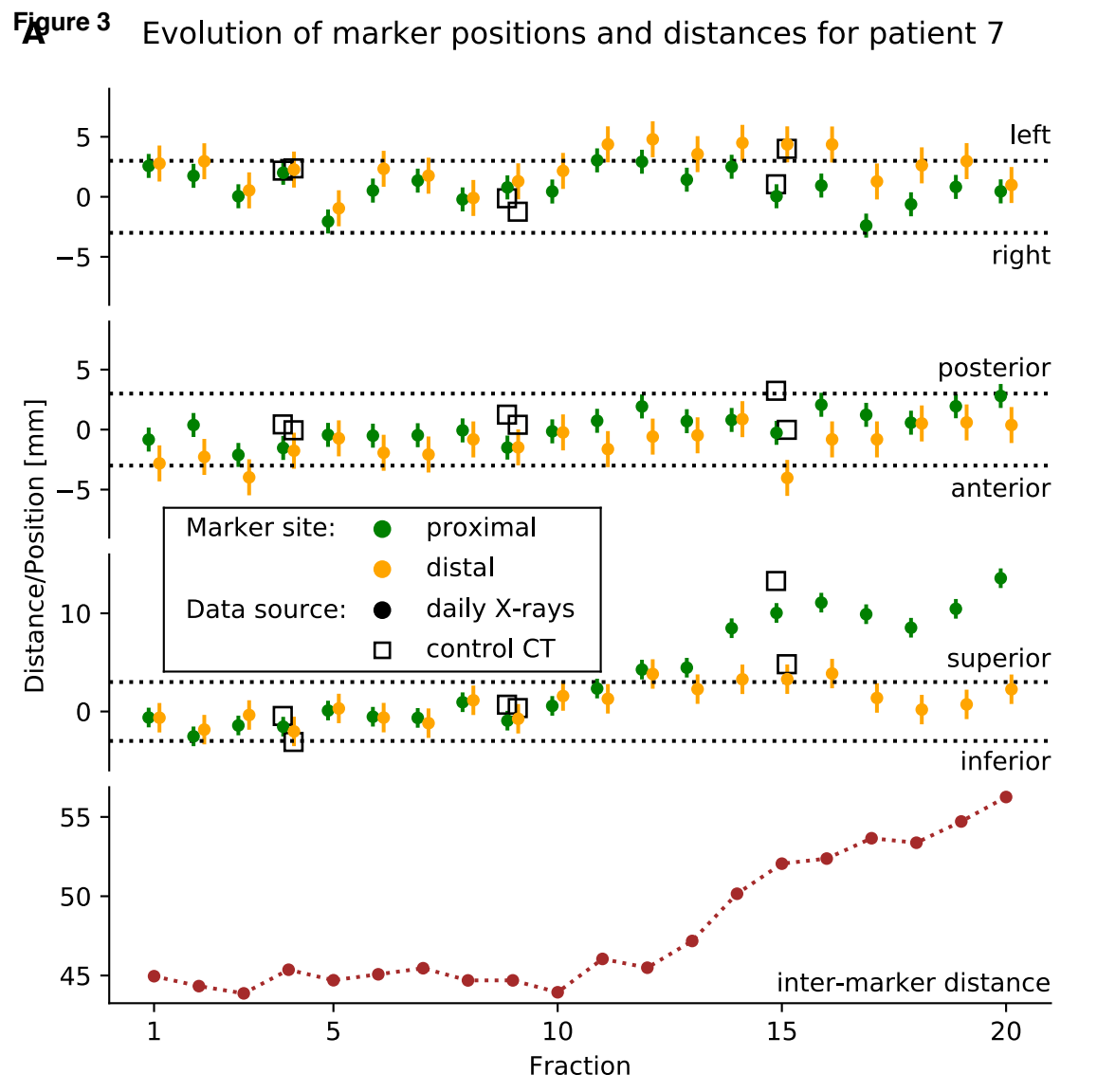
A
Evolution of marker positions and distances for patient 7
left
right
posterior
anterior
superior
inferior
Distance/Position [mm]
Marker site:
proximal
distal
Data source:
daily X-rays
control CT
inter-marker distance
Fraction

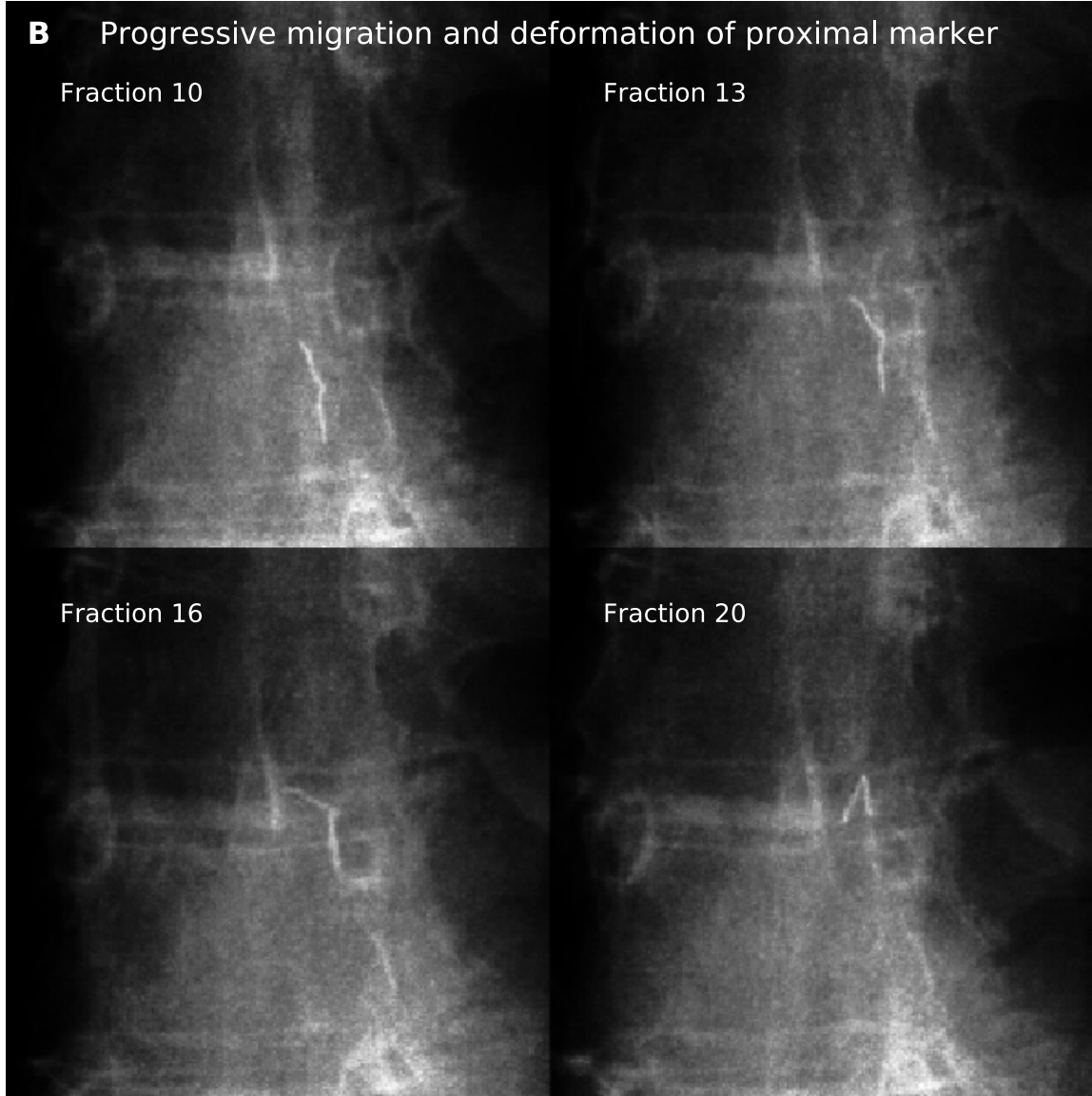
B
Progressive migration and deformation of proximal marker
Fraction 10
Fraction 13
Fraction 16
Fraction 20

Figure 4

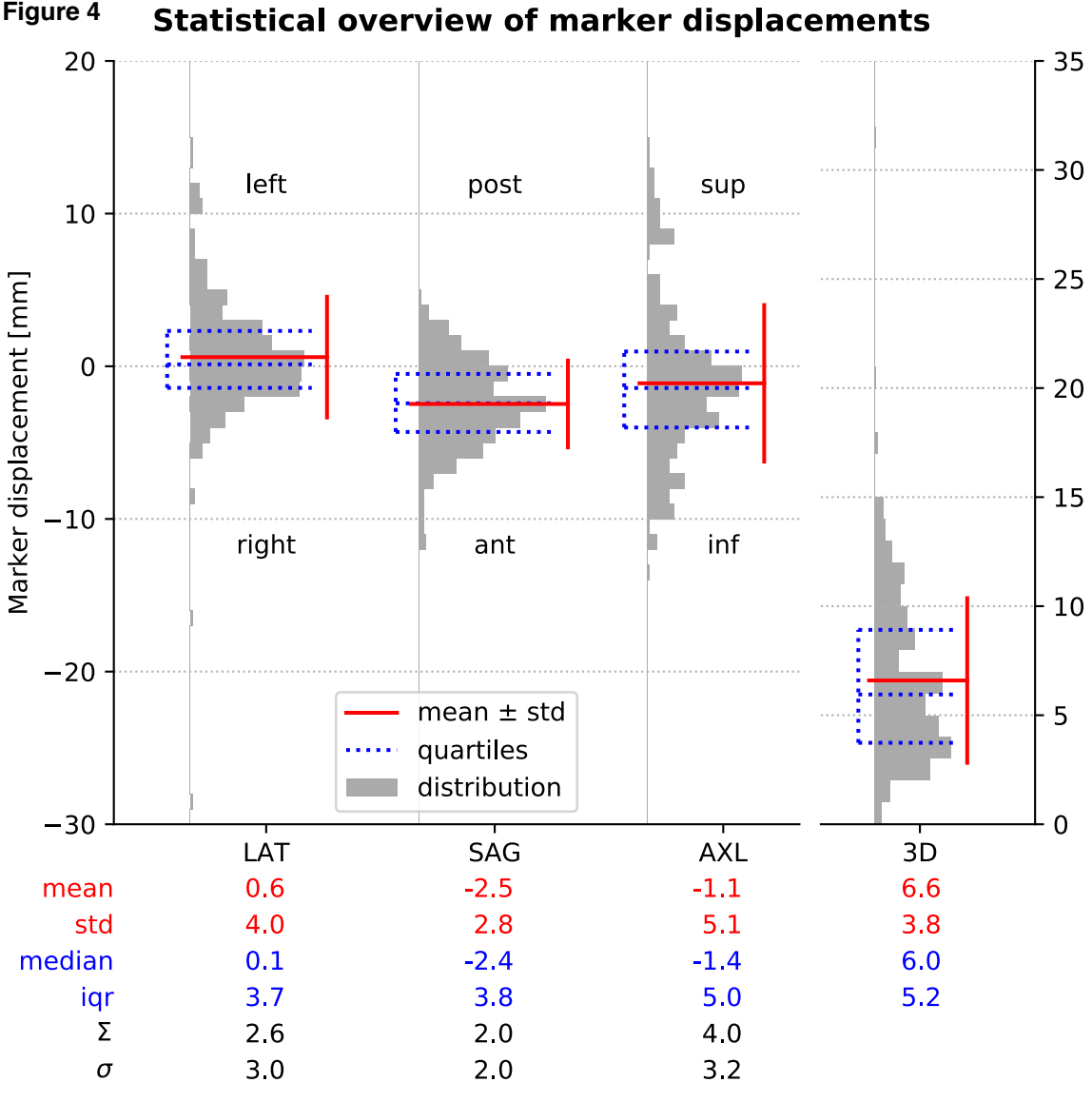
Statistical overview of marker displacements
Marker displacement [mm]
20
10
0
−10
−20
−30
35
30
25
20
15
10
5
0
left
post
sup
right
ant
inf
mean ± std
quartiles
distribution
LAT
SAG
AXL
3D
mean 0.6 -2.5 -1.1 6.6
std 4.0 2.8 5.1 3.8
median 0.1 -2.4 -1.4 6.0
iqr 3.7 3.8 5.0 5.2
Σ 2.6 2.0 4.0
σ 3.0 2.0 3.2

Figure 5

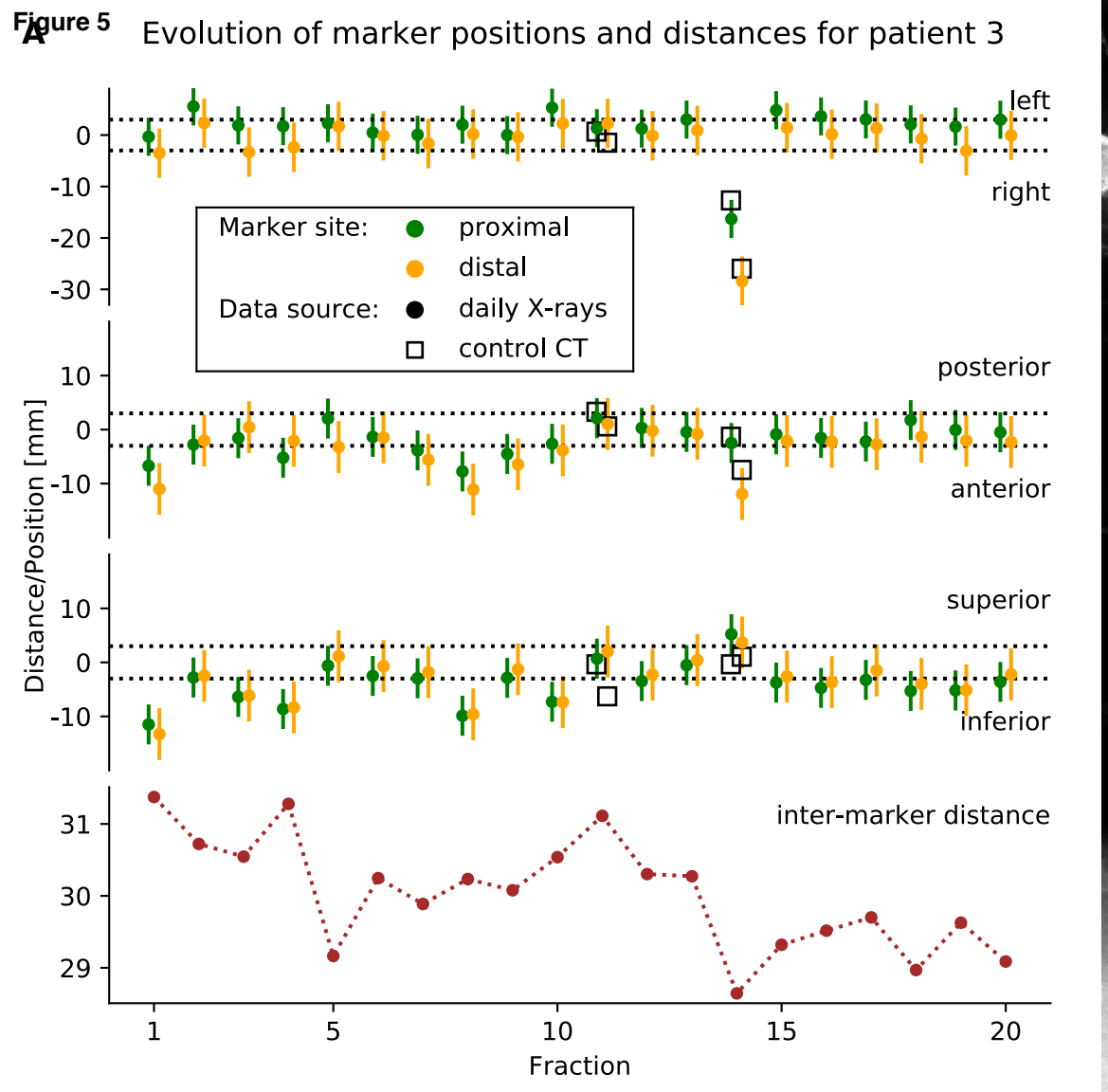
A
Evolution of marker positions and distances for patient 3
left
right
posterior
anterior
superior
inferior
inter-marker distance
Marker site:
proximal
distal
Data source:
daily X-rays
control CT
Distance/Position [mm]
Fraction

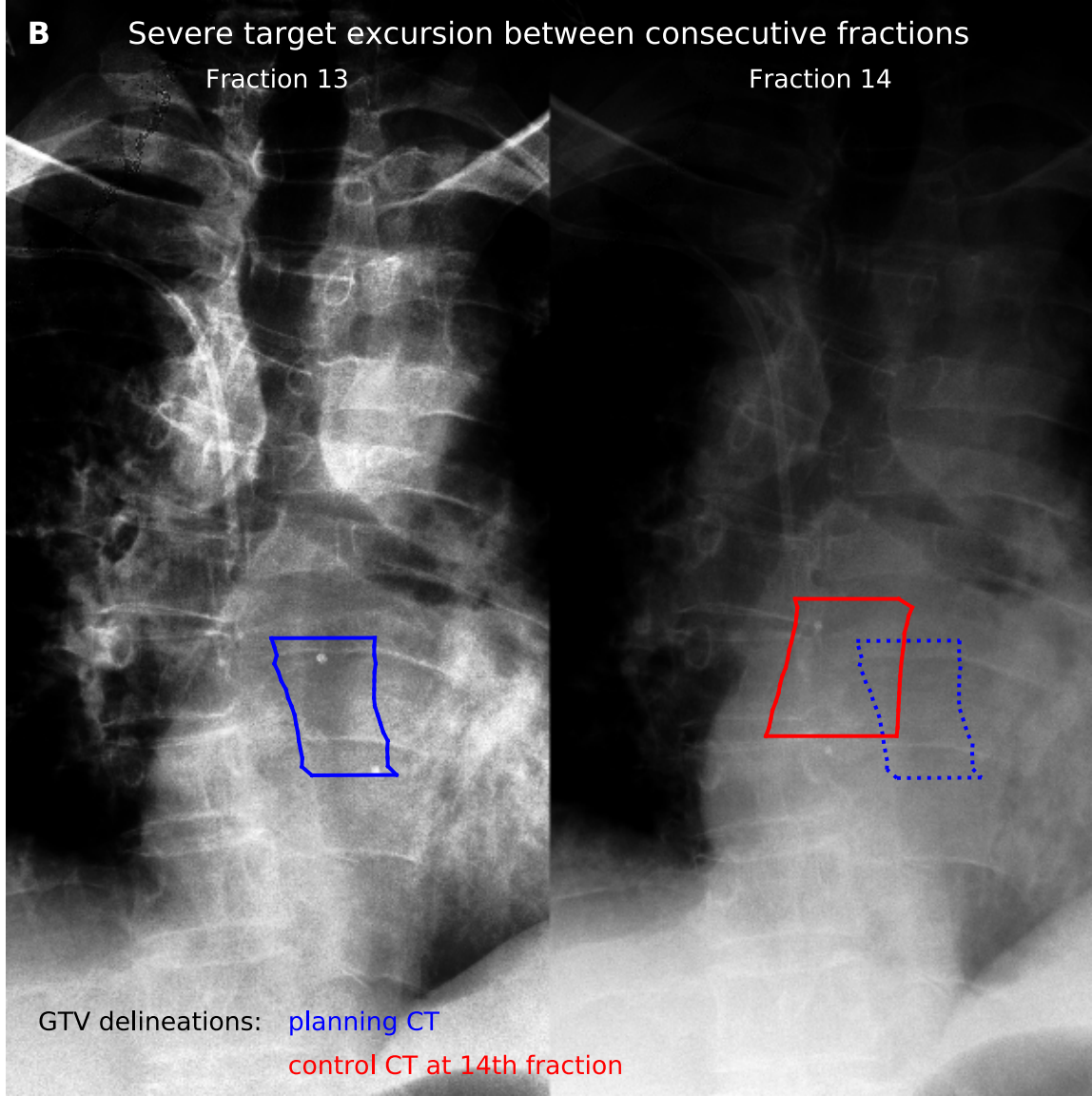
B
Severe target excursion between consecutive fractions
Fraction 13
Fraction 14
GTV delineations:
planning CT
control CT at 14th fraction